Impact of material property variations and sensor positioning on the coating thickness determination of steel sheets using eddy current testing

Martin Koll, Daniel Wöckinger, Christoph Dobler, Gereon Goldbeck, Gerd Bramerdorfer, Stefan Schuster, Stefan Scheiblhofer, Norbert Gstöttenbauer and Johann Reisinger
(Author affiliations can be found at the end of the article)

COMPEL – The international journal for computation and mathematics in electrical and electronic engineering

355

Received 9 October 2024
Revised 18 November 2024
Accepted 3 December 2024

Abstract

Purpose – This paper aims to investigate the reliable thickness, and more generally, the geometric and material parameter determination of thin electrically conductive and diamagnetic coatings on conductive and ferromagnetic substrates, e.g. steel, using eddy current testing (ECT).

Erratum: It has come to the attention of the publisher that the article Koll, M., Wöckinger, D., Dobler, C., Goldbeck, G., Bramerdorfer, G., Schuster, S., Scheiblhofer, S., Gstöttenbauer, N., & Reisinger, J. (2024). "Impact of material property variations and sensor positioning on the coating thickness determination of steel sheets using eddy current testing". *COMPEL – The international journal for computation and mathematics in electrical and electronic engineering*. https://doi.org/10.1108/COMPEL-10-2024-0415, contained several errors:

1. The affiliation "Institute for Electrical Drives and Power Electronics" has been corrected to "Institute of Electric Drives and Power Electronics."
2. There was an error in Formula (1). The correct formula is as follows:

$$\zeta = \frac{\mathrm{j}\omega\mu_0\pi N_1 N_2 \bar{r}}{(r_2 - r_1)(r_4 - r_3)L_2 L_6} \int_0^\infty \frac{1}{\alpha^6} J(r_2, r_1) J(r_4, r_3) e^{-2\alpha L} \left(e^{-\alpha(L_2 - 2L_5 - L_6)} - 1\right) \times \left(e^{-\alpha L_5} - e^{-\alpha(L_6 + L_5)}\right)\left(e^{-\alpha L_2} - 1\right) \frac{(\alpha+\beta_1)(\beta_1-\beta_2) + (\alpha-\beta_1)(\beta_1+\beta_2)e^{2\alpha_1 c}}{(\alpha-\beta_1)(\beta_1-\beta_2) + (\alpha+\beta_1)(\beta_1+\beta_2)e^{2\alpha_1 c}} \, \mathrm{d}\alpha. \quad (1)$$

3. An incorrect degree sign was present in the second line of Table 1 in the formula: min(16/L mm^2 …). This degree sign has now been removed.
4. There was an error in the unit measurements. μm has now been corrected to µm.

These errors were introduced during the production process. The publisher sincerely apologises for these errors and for any confusion caused.

This work has been supported by the COMET-K2 "Center for Symbiotic Mechatronics" of the Linz Center of Mechatronics (LCM) funded by the Austrian federal government and the federal state of Upper Austria.

COMPEL – The international journal for computation and mathematics in electrical and electronic engineering
Vol. 44 No. 3, 2025
pp. 355-371
Emerald Publishing Limited
0332-1649
DOI 10.1108/COMPEL-10-2024-0415

Design/methodology/approach – The analytical model of an ECT coil arrangement known from the literature is analyzed to evaluate the numerical simulation performed by a Finite Element (FE) program. The latter is used to investigate the influence of the sheet edge on the measurement result. Finally, a measurement setup is presented and the unknown geometric and material parameters are estimated from measurement data of different sample sheets at different air gaps.

Findings – Generally, valid mesh rules are found for a very accurate FE analysis of eddy current problems with large air gaps. The influence of large air gaps on the parameter estimation is emphasized. Moreover, the formulated hypotheses can be widely confirmed by measurements.

Research limitations/implications – In this paper, electrical steel sheets coated with a conductive oven-cured ink are used. This sample configuration creates a discrete transition between the substrate and the coating as present in the analytical modeling approaches. Furthermore, the ferromagnetic substrate's nonlinear B-H curve is not considered in the analytical model so far.

Originality/value – The analytical model is known from the literature. However, real practical measurements have not been carried out with the discussed setup. Furthermore, well-known literature on eddy current measurements usually only considers constant and very small air gaps.

Keywords Eddy current testing, Finite element analysis, Nondestructive testing, Magnetic nonlinearity, Electromagnetic fields

Paper type Research paper

1. Introduction and methodology

Coatings are typically applied to steel sheets to protect them against external influences that could damage the material, e.g. corrosion. For an inline quality monitoring of the coating, it is essential to accurately determine the coating parameters, e.g. coating thickness and its material composition. Thus, the specified coating properties can be guaranteed. According to the literature, an X-ray gauge is often used to determine coating thicknesses inline (Moriyasu *et al.*, 2018). This method is typically costly and poses problems in terms of occupational safety. An eddy current coil system is used for the following investigations as an inexpensive and safe promising alternative. In industry, eddy current testing is widely applied for nondestructive investigations of various steel products. Due to the harsh industrial process conditions, e.g. high temperature and ferrous dust, the eddy current measuring coils need a safety distance of some millimeters to centimeters away from the steel strips. In addition, sheet vibrations in continuous industrial processes, as shown as dashed lines in Figure 1, can occur and result in local liftoff variations at the measurement location. The parameter $L_{\min}$

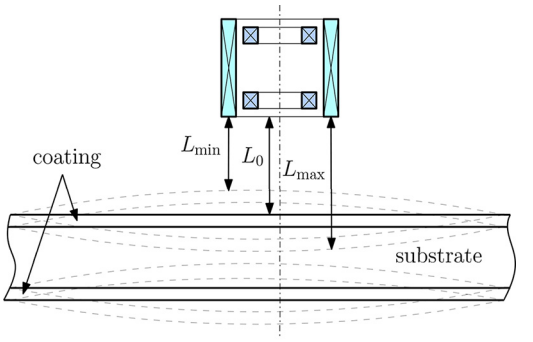

Source: Authors' own work

Figure 1. Schematic drawing of the selected ECT system with liftoff variations in a potential industrial process

denotes the minimum and L_{max} the maximum air gap between the sheet surface and the coil system. In general, eddy current sensor measurements are based on inducing eddy currents in conductive materials and evaluating the interaction with the applied field. The feedback is then used to determine the object's material properties. For this reason, the paper investigates a model-based method for reliable coating thickness determination. The relevant analytical model is known from the literature (Dodd, 1969). The coil arrangement used in this paper is shown in Figure 2. It consists of an external solenoid excitation coil and two solenoid measuring coils wound in opposite directions, whereby only the differential voltage is evaluated. This coil system has been chosen, as the typically temperature-dependent ohmic resistance of the excitation coil does not impact the measurement result. Furthermore, this coil system provides zero output voltage if no electrically conductive object is nearby. The advantage of this type of sensor coil is that changes in the electrical and magnetic properties of the object to be measured have a direct effect on the measurement voltage. To confirm the validity of the analytical model and the validity ranges about the distance of the coil to the sheet's edge, finite element (FE) simulations are carried out using the software FEMM (Meeker, 2024). FEMM is limited to two-dimensional (2D) problems. This is sufficient for the investigations carried out in this paper. It is assumed that no tilting between the coil and the sheet occurs. Furthermore, the sheet properties are considered to be isotropic, linear and homogeneous. Thus, rotational symmetry is fulfilled and the three-dimensional problem can be treated as a 2D problem. Therefore, generally valid mesh rules for layered eddy current problems are specified and evaluated. In addition, a robustness analysis with regards to undesired parameter variations is carried out. A measurement setup is presented for investigating various coated sheet metal samples with coating thicknesses ranging from 8 to 21 µm. Furthermore, the influence of air gap variations on the measurement result is investigated. The unknown material parameters are finally estimated and analyzed based on the acquired measurement data using the previously mentioned model-based estimation approach. Thereby, the influence of air gap variations on the estimation result is examined.

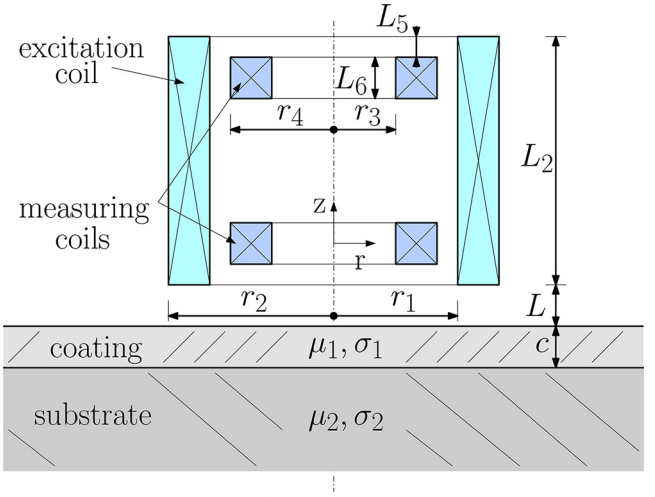

Source: Authors' own work

Figure 2. Selected ECT coil system for measuring coated steel sheets with its dimensions

2. Analytical model

Based on Dodd (1969) the mutual impedance ζ of the coil arrangement in Figure 2 is:

$$\zeta = \frac{\mathrm{j}\omega\mu_0\pi N_1 N_2 \bar{r}}{(r_2 - r_1)(r_4 - r_3)L_2 L_6} \int_0^\infty \frac{1}{\alpha^6} J(r_2, r_1) J(r_4, r_3) e^{-2\alpha L} \left(e^{-\alpha(L_2 - 2L_5 - L_6)} - 1\right) \times \left(e^{-\alpha L_5} - e^{-\alpha(L_6 + L_5)}\right)\left(e^{-\alpha L_2} - 1\right) \frac{(\alpha+\beta_1)(\beta_1-\beta_2) + (\alpha-\beta_1)(\beta_1+\beta_2)e^{2\alpha_1 c}}{(\alpha-\beta_1)(\beta_1-\beta_2) + (\alpha+\beta_1)(\beta_1+\beta_2)e^{2\alpha_1 c}} \,\mathrm{d}\alpha. \tag{1}$$

Note that for the considered analytical modeling approach linear, isotropic and homogeneous material is assumed for all sheet layers. Here, $\omega = 2\pi f$ is the angular excitation frequency, N_1 and N_2 are the number of turns of excitation and measuring coils, respectively. Furthermore, r_i and L_i are the dimensions of the respective coils and the relationships:

$$\bar{r} = \frac{r_1 + r_2}{2}, \tag{2}$$

$$\beta_i = \frac{1}{\mu_i}\sqrt{\alpha + \mathrm{j}\overline{r^2}\omega\mu_0\mu_i\sigma_i}, \tag{3}$$

$$\alpha_i = \sqrt{\alpha + \mathrm{j}\overline{r^2}\omega\mu_0\mu_i\sigma_i}, \tag{4}$$

$$\frac{1}{\alpha^2}\int_{x=\alpha r_1}^{\alpha r_2} x J_1(x)\,\mathrm{d}x = \frac{1}{\alpha^2} J(r_2, r_1), \tag{5}$$

with $J_1(x)$ the Bessel function of first kind and first order are needed. The layers' relative permeability and conductivity are defined as μ_i and σ_i. Because the coating is diamagnetic, $\mu_1 = 1$. The integration variable of the infinite integral in equation (1) is specified to α. The computing time of one run of the analytical model is approximately 110 ms in MATLAB (MathWorks, 2024) using an Intel i9-10900F. These model equations are valid for analyzing the materials two-layer structure. However, it can be extended to a multilayer structure (Luquire *et al.*, 1970). In these models, it is assumed that the material properties, e.g. the conductivity and permeability of the layers, are constant. In Uzal and Rose (1993), a continuous variation of the conductivity in a layer is investigated through piecewise approximations by introducing a large number of sublayers. In contrast, in Theodoulidis *et al.* (1995) analytical solutions for selected continuous conductivity distributions are presented.

Figure 3 shows the frequency *locus* of the mutual impedance ζ generated based on the two-layer analytical model, equations (1) to (5), for three different settings with different coating thicknesses c_i and air gaps L_i. The material parameters used are $\sigma_1 = 15$ MS/m, $\sigma_2 = 5$ MS/m and the constant relative permeability $\mu_2 = 500$. Due to the assumption of linear, isotropic and homogeneous sheet materials, the magnitude of the current does not impact the frequency locus of the mutual impedance. These frequency locus curves are valid for a radially infinitely extended sheet. For this reason, the following section analyses up to which sheet radius the model provides results of reasonable accuracy. The mutual impedance ζ can be determined from measurements with:

$$\zeta = \frac{U_{\mathrm{diff}}}{I}, \tag{6}$$

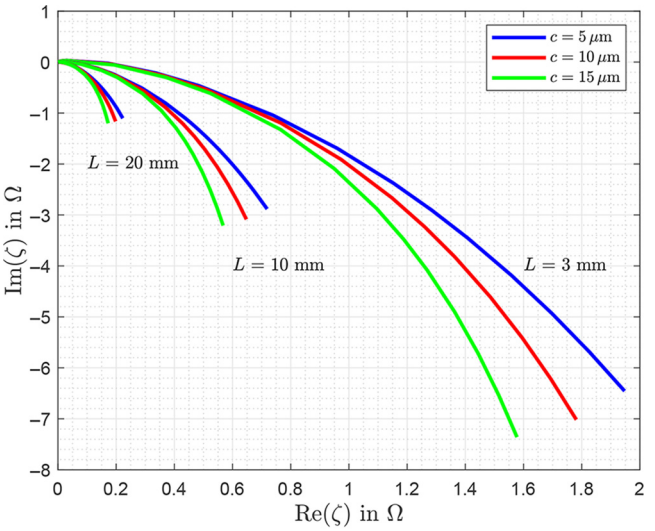

Source: Authors' own work

Figure 3. Frequency locus of the mutual impedance for different air gaps L and coating thicknesses c_i at frequencies f = [100 Hz–200 kHz] calculated with the analytical model

where U_{diff} is the complex differential voltage between the two measuring coils including magnitude and phase, and I is the excitation current magnitude.

3. Finite element verification of the analytical model and consideration of the edge effect

As aforementioned, for the analytical model it is assumed that the sheet metal is of infinite extension in radial direction. In practice, this assumption is never fulfilled. To find the limits of the analytical model, a so-called edge effect simulation based on an FE analysis is performed. Figure 4 shows a schematic representation of the coil system under investigation in FEMM (Meeker, 2024). To give an insight into geometric dependencies, four different coil setups with different parameter settings are analyzed. This investigation aims to determine the necessary minimum distance between the coil system and the edge of the sheet as a function of the air gap, ensuring that the edge effect in the resulting mutual impedance is practically negligible. Therefore, the sheet metals and coating's electrical parameters are set to σ_1 = 15 MS/m and σ_2 = 5 MS/m, the analyzed coating thickness is defined to be c = 10 µm and the substrate's constant relative permeability is μ_2 = 500. These are typical parameters for materials to be coated. Furthermore, the dependency on the coils' geometry is evaluated for air gaps up to L = 100 mm. Typically, very fine meshes are required to cover the eddy current problem with sufficient accuracy due to the small penetration depths at high frequencies. This leads to a dramatic increase in the number of finite elements and, hence, in computing time. To reduce the latter, the computational domain is subdivided into individual regions and separate mesh rules are introduced for each region. In Figure 5, six defined mesh regions are visible in the 2D representation in FEMM. Region 1 is called the outer air region. This region separates the more finely meshed Region 2 from the outer boundary of the

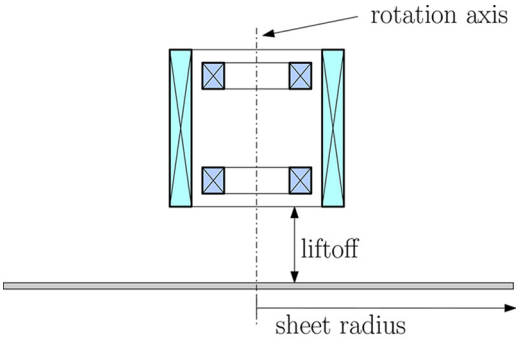

Source: Authors' own work

Figure 4. Schematic representation of the edge effect simulation setup depending on the sheet radius and the liftoff

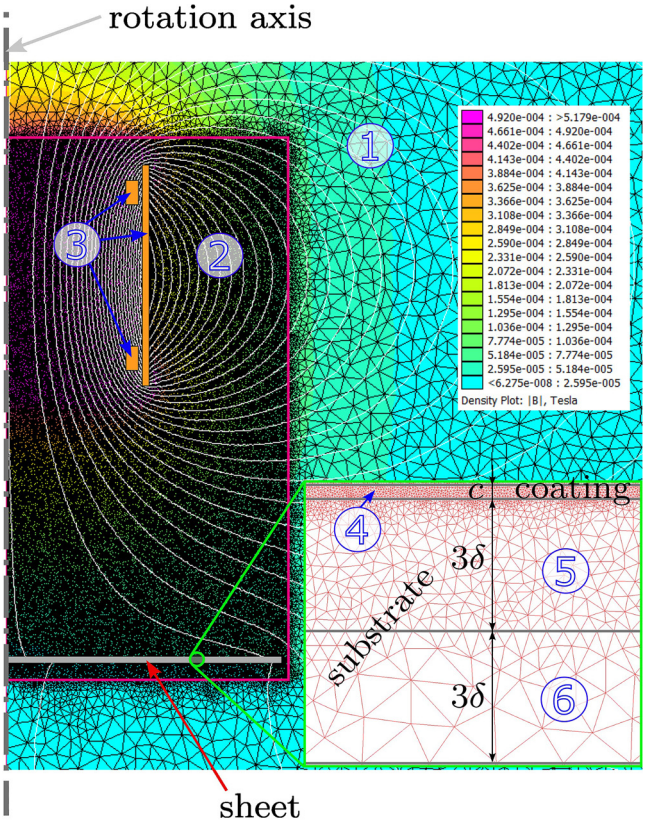

Source: Authors' own work

Figure 5. The computing domain featuring different mesh regions, where the magnetic field and the mesh for an excitation frequency of $f = 100$ kHz are visualized

problem. Region 2 is called the inner air region. The red line separates Region 1 from 2. Region 3 corresponds to the coil system. The sheet metal is divided into three regions, called 4, 5 and 6. On the one hand, Region 4 describes the coating. On the other hand, Regions 5 and 6 divide the substrate into two areas. Concerning Region 5, the maximum mesh length is calculated as a function of the penetration depth according to the well-known equation for evaluating the skin effect in linear material:

$$\delta = \sqrt{\frac{2}{\omega \mu_0 \mu_i \sigma_i}}. \tag{7}$$

In contrast, the top substrate layer 5 is modeled three times the penetration depth, whereas the bottom substrate layer 6 is used to create a variable sheet thickness. As the frequency increases, the penetration depth decreases and the physical sheet thickness can be reduced without impacting the simulation result. This saves nodes and, thus, computing time, as the substrate area can be modeled smaller without causing a noticeable error. For example, with an excitation frequency of $f = 200$ kHz and the sheet substrate parameters $\mu_2 = 500$ and $\sigma_2 = 5$ MS/m, the sheet thickness only needs to be modeled as 22 µm thick. The air gap–based mesh rule presented in Table 1 is used for the air region 2 around the coil. With the mesh rules shown in Table 1, a relative error of $\epsilon < 0.04\%$ between the analytical model and the FE simulation is achieved if the sheet radius is sufficiently large. The true value of the mutual impedance is defined by the analytical model. The FEMM built-in smart mesh option is used in regions without a specified mesh rule. As mentioned above, edge effect simulations are carried out to investigate the influence of the sheet metal edge on the mutual impedance. For this purpose, the sheet radius is varied at different air gaps and compared with the solution of the analytical model. The result is the error plot in Figure 6 as a function of the liftoff and the sheet radius.

Table 2 shows the coil setups' parameters investigated. The investigated coil's size decreases from setup 1 to setup 4. From Figure 6, it is observed that the relative error increases as the liftoff increases and the sheet radius decreases. This provides a guide for the practical positioning of the sensor system to avoid a significant edge effect. It can be seen that at large air gaps, the error caused by the edge effect can only be reduced to a limited extent, e.g. 1% error relative to the analytical model at a liftoff of 100 mm and a sheet radius of 100 mm, by using the smaller coil setup 4. In contrast, coil setup 1 requires a minimum sheet radius of 150 mm for the selected sheet with a liftoff of 50 mm to reduce the error due to the edge effect to less than 1%. The computing time of an operating point at $f = 100$ kHz on an Intel i9-10900F with the selected mesh rules is approximately 10 min. The geometric limitations with regard to the

Table 1. Mesh rules used in the defined regions 1–6 in the 2D-FE simulation in FEMM

Region name	Nr.	Setting for max. mesh size
Outer air	1	3 mm (FEMM smart-mesh)
Inner air	2	$\min(\frac{16}{L}\text{mm}^2, 1\text{mm})$
Coil system	3	0.02 mm (FEMM smart-mesh)
Coating	4	$c/5$
Sheet top layer	5	$\delta/3$
Sheet bottom layer	6	0.1 mm (FEMM smart-mesh)

Source: Authors' own work

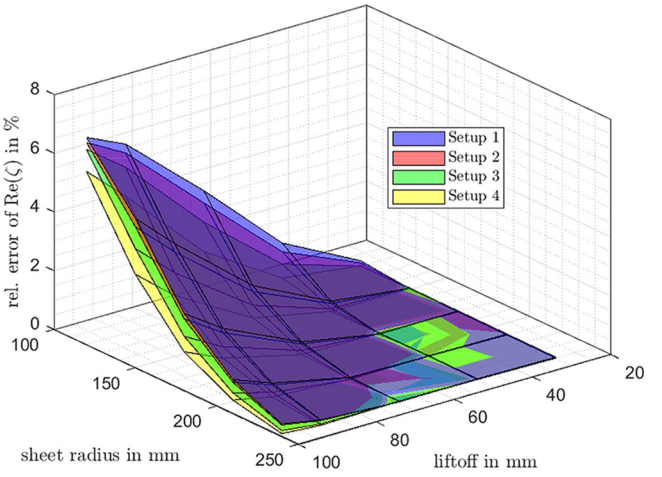

Source: Authors' own work

Figure 6. Relative error of the real part of the mutual impedance between the analytical model and the FE simulation at $f = 100$ kHz depending on the sheet radius and liftoff

Table 2. Used coil setups to consider the edge effect and its dimensions in millimeter

	Setup 1	Setup 2	Setup 3	Setup 4
r_1 [mm]	25	13	25	10
r_2 [mm]	26	14	26	11
r_3 [mm]	22	10	22	7
r_4 [mm]	24	12	24	9
L_2 [mm]	40	40	20	10
L_5 [mm]	2.85	2.85	2.85	1.5
L_6 [mm]	4.1	4.1	4.1	3

Source: Authors' own work

setup's practical positioning of the analytical model have now been found and further investigations, e.g. its robustness against material parameter variations, can be carried out.

4. Robustness analysis

Previous research with different approaches has demonstrated that it is impossible to determine the coating thickness and its conductivity independently of each other (Moulder *et al.*, 1992; Ptchelintsev and de Halleux, 1996; Ptchelintsev and de Halleux, 1998). The same applies to the substrate permeability and substrate conductivity. This effect is independent of the coil geometry, e.g. a coil with a rectangular cross section, a single solenoid or a coil system consisting of an excitation coil and a measuring coil (Koll *et al.*, 2024). In this paper, the focus is primarily on determining the coating thickness. Therefore, the robustness analysis is limited to coating conductivity and thickness variation. The robustness analysis is carried out by making use of the analytical model with a magnetically linear ferromagnetic substrate. The

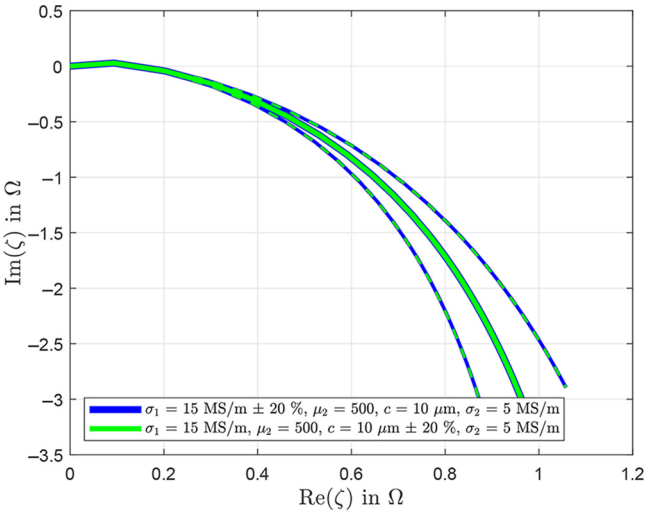

Source: Authors' own work

Figure 7. Results of a robustness analysis regarding coating thickness and coating conductivity variation illustrated in the complex frequency locus curve

results of a coating thickness change of ± 20% and a coating conductivity variation with the same relative variation are plotted in Figure 7 as a tube around the initial frequency *locus* curve from $f = 100$ Hz to $f = 200$ kHz at a fixed liftoff of $L = 10$ mm as dashed lines. It can be seen that a 20% increase in conductivity has the same effect on the frequency *locus* curve as a 20% increase in coating thickness. Accordingly, it is essential to know the conductivity of the coating to determine the coating thickness accurately from measurement data. Note that the discussed behavior is similar for all air gaps and coil setups.

5. Measurement setup

Eddy current measurements are often carried out using impedance analyzers. However, this paper presents a self-developed test rig for measuring coated sheet metal samples to be able to impress various current magnitudes into the excitation coil. Figure 8 shows a block diagram of the measurement setup and the main signal paths. A measurement PC is used to perform sinusoidal signal generation, analysis and the superimposed iterative current control. The

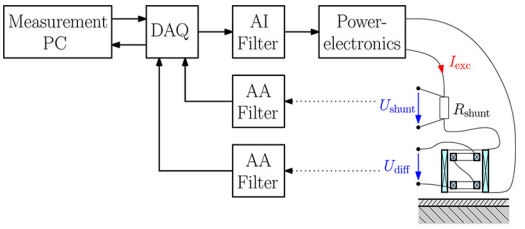

Source: Authors' own work

Figure 8. Block diagram of the measurement setup

connection to the hardware is made via a National Instruments – USB – 6356 data acquisition (DAQ) (NI-USB–6356, 2024) box with a fixed sample rate of 1.25 MS/s per channel. An anti-imaging filter for signal smoothing is applied because sinusoidal excitation current frequencies of over 180 kHz are used. Both, the antialiasing and the anti-imaging filter consist of an upstream impedance converter and a downstream active second-order low-pass filter designed in Sallen-Key topology (Sallen and Key, 1955). The cut-off frequency of the filter is set to approximately f_c = 600 kHz, which is roughly half the sampling frequency of the DAQ box. Furthermore, a linear power amplifier, i.e. ServoWatt DCP520/84 HSR (DCP 520/84 HSR, 2024), is used. The advantage of such a power electronics is that its properties, e.g. gain and frequency behavior, can be set via an external easy-to-adapt circuit board. Generally, analog current control would be the best, ensuring the current is as sinusoidal as possible. However, due to the high excitation frequencies, it is not straightforward to implement a stable analog current control. As the coil shows approximately linear magnetic behavior, it is also possible to operate the power electronics as a voltage–voltage amplifier with a superimposed iterative current control, which is much easier to put in to operation. The assumption of linear magnetic coil characteristics follows sufficient accuracy, as the coil is not surrounded by a high-permeable iron core and the liftoff between solenoid and sheet is high. The purpose of the iterative current control is to adjust the output voltage of the DAQ box in each iteration step, until the target current magnitude and the predefined signal quality is reached. An inverting voltage-voltage amplifier with gain $v = -10$ is selected for the later presented measurement results. In addition, a shunt resistor R_{shunt} = 33 mΩ is used for an indirect current measurement. As the shunt has a non-negligible phase shift between its current and voltage at high excitation frequencies, the current cannot be directly calculated by using the afore introduced resistance value. Instead, frequency-dependent shunt characteristics must be determined. This allows to accurately derive the current based on the shunt voltage measurement. For efficient postprocessing, the measured current and the differential voltage between the two measuring coils are then represented in terms of frequency components by applying the Fast Fourier Transform (Cooley and Tukey, 1965). The fundamental wave Fourier coefficients of the measured voltage and current are extracted and the mutual impedance value $\zeta(f)$ associated with the respective frequency is calculated by using equation (6) Figure 9 shows the manufactured sample holder for the sheet

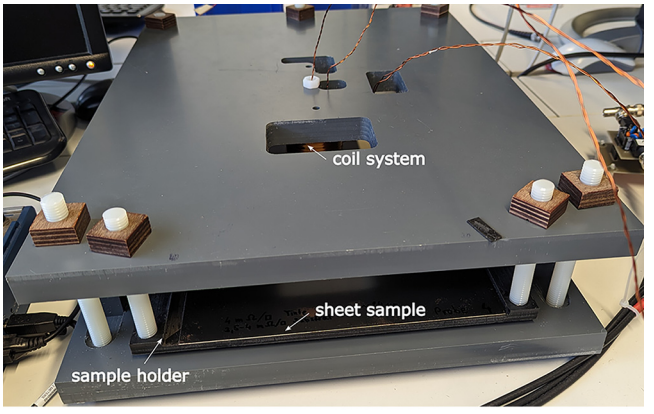

Source: Authors' own work

Figure 9. Sheet sample holder with an uncoated substrate sample inserted

metal samples. It is made of electrically and magnetically nonconductive plastics and wood and can be used to set air gaps between $L = 1$ mm and $L = 25$ mm. The coil system is placed in the center of the test rig. The sheet metal samples to be measured are 400 × 200 × 0.5 mm in size. Referring to the results in Section 3, there is no noticeable edge effect in the measurement results if coil setup 1 is used. Because coil setup 1 has the largest geometric expansion, the other coil setups, i.e. 2–4 in Table 2, can also be used for these sheet metal samples and air gaps. For the air gaps under consideration, a relative error of less than 0.1% to the analytical model can thus be ensured with regard to the edge effect. The substrate of the samples consists of an M800-50A electrical steel sheet, and the coating is a silver ink Loctite EDAG PF 410 E&C (LOCTITE EDAG PF 410 E&C Datasheet, 2024) that is screen-printed onto the substrate and then cured in an oven. Due to this production process, the substrate material cannot be fully coated to its edge. This ink is usually used to print flexible circuits, e.g. for small and precise heating systems. It was chosen here to obtain the best possible setting for verifying the analytical model by means of measurements. For instance, using this ink ensures a discrete transition between the substrate and the coating, which fulfills the model requirements well. This sharp transition cannot be achieved in an industrial coating process in this form, as the sheet metals to be coated have a certain roughness, and alloy formation occurs at the transitions. One of these coated sheet metal samples is shown in Figure 10. The sheet metal samples are thus defined, and a test setup is made available. The next step is to measure these samples and determine the unknown parameters.

6. Measurement results

As already mentioned, it is impossible to determine all five sheet metal parameters independently based on the measurement data that can be obtained. For this reason, the substrate and coating conductivity are measured in advance. The substrate conductivity is determined using a van der Pauw measurement (Pauw, 1958). The coating conductivity is known from experience and reference measurements from other applications. The results for the conductivities are $\sigma_1 = 6.94$ MS/m and $\sigma_2 = 3.054$ MS/m. In this paper, three coated samples with different coating thicknesses (c_1, c_2 and c_3) in the range of 8, 12 and 21 µm are analyzed. Figure 11 shows the frequency *locus* curves of the different samples at different air gaps for a frequency sweep from $f = 460$ Hz to $f = 183$ kHz. The current magnitude was controlled to $\hat{I} = 0.2$ A at each operating point to obtain comparable results. The current can be controlled to an accuracy of ± 0.01% with the selected measurement setup, control concept and excitation current. The number of turns of the primary and secondary windings of the assembled coil setup 1 are $N_1 = 43$ and $N_2 = 18$. In Figure 11, different layer thicknesses are easily recognizable and distinguishable. The unwanted kink in the green curve at small liftoff is due to the measuring range switching in the DAQ box. The analytical model assumes ferromagnetic material with a linear B-H curve in the substrate. In reality, however, the effective permeability depends on the magnetic field applied to the material. Therefore, the magnetic operating point can be influenced by the excitation current or by a change in the air gap. Different current magnitudes are studied for a specific constant air gap between the sheet sample and the coil system to evaluate this influence. The results in Figure 12 show that the frequency *locus* curve moves to the top right as the current increases. Note that the linear analytical model interprets this change as a permeability increase of the substrate material in the so-called Rayleigh range (Rayleigh, 1887) of ferromagnetic materials with non-linear B-H dependence. This assumption is valid because the air core excitation coil can only generate a maximum magnetic flux density of a few milli Tesla in the substrate material.

Thus, measurement data for different sheet samples is available for different air gaps, different current magnitudes and, therefore, different magnetic operating points. The nonlinear effects caused by varying the current magnitude are clearly recognizable in

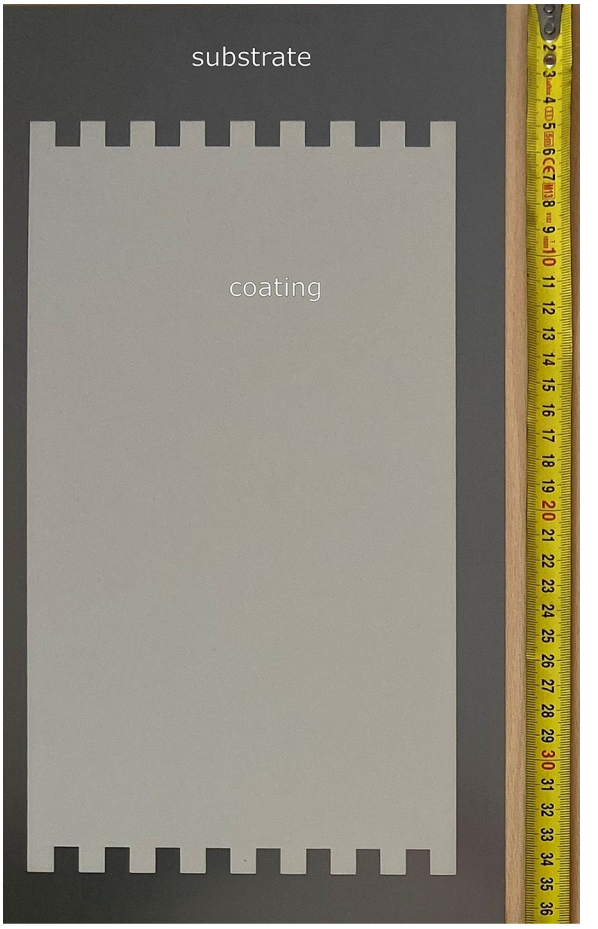

Source: Authors' own work

Figure 10. M800 – 50A sheet sample with oven-cured highly conductive ink EDAG PF 410 E&C used as coating

Figure 12. In Section 7, the unknown material parameters will be determined using estimators, and the influence of the ferromagnetic substrate with nonlinear B-H dependence on the parameter estimation is demonstrated.

7. Parameter estimator

Typically, the unknown parameters are the liftoff L, the coating thickness c and the constant relative permeability μ_2, which depends on the set magnetic operating point. As previously described, it is assumed that the conductivities σ_1 and σ_2 are known in advance. To identify these parameters based on measuring data, a least squares problem with a cost function:

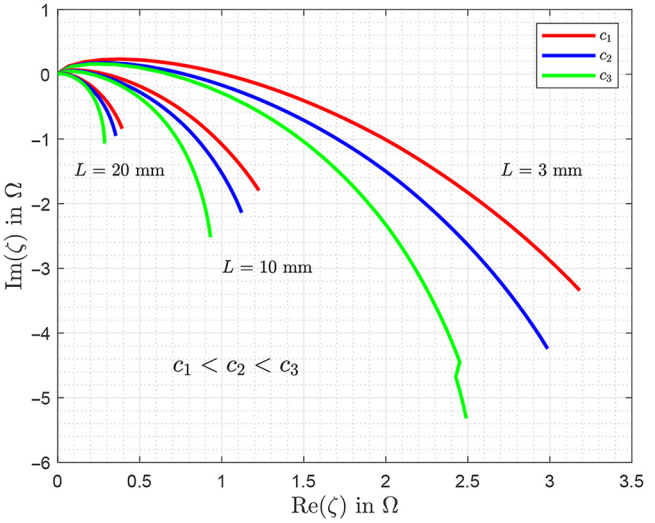

Source: Authors' own work

Figure 11. Frequency locus curves of different sheet metal samples measured at different air gaps with an excitation current $\hat{I} = 0.2$ A

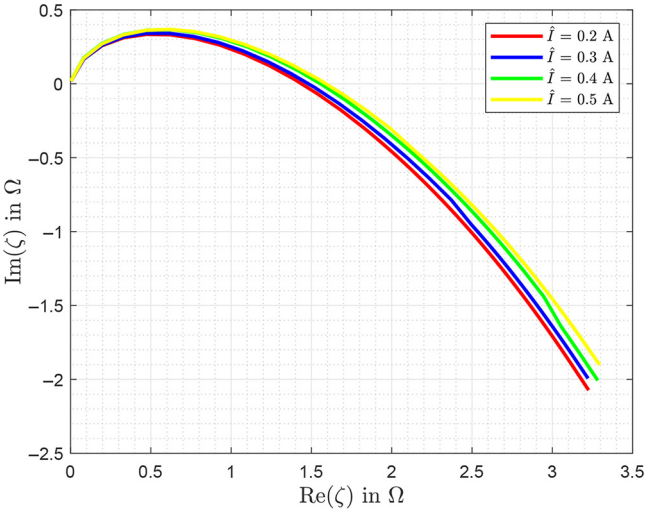

Source: Authors' own work

Figure 12. Frequency locus curves of constant airgap $L = 3$ mm and coating thickness c_1 evaluated at different excitation current amplitudes $\hat{I}$

$$J(c, L, \mu_2, f) = \sum_{f_{\max}}^{f_{\min}} \left(\zeta_{\text{meas}}(c, L, \mu_2, f) - \zeta_{\text{model}}(c, L, \mu_2, f)\right)^2 \tag{8}$$

is used. $\zeta_{\text{meas}}(c, L, \sigma_1, \mu_2, \sigma_2, f)$ denotes the frequency *locus* curve of the mutual impedance determined for all measurement frequencies. The frequency range specified in Section 6 is also considered for the estimation problem. Generally, by minimizing this cost function:

$$\left(\widehat{c}, \widehat{L}, \widehat{\mu}_2\right) = \underset{c, L, \mu_2}{\operatorname{argmin}}(J), \tag{9}$$

an estimate of the unknown parameters can be obtained. Because the used cost function J is smooth and has no local minima, a gradient-based method is suitable for solving this minimization problem.

Table 3 shows the parameter estimation results, including the coating thickness and the air gap length at the different air gaps considered. Figure 13 shows the effective relative permeability estimation results for the various air gaps under consideration.

The layer thickness estimation tends to deviate slightly as the air gap increases. This can be explained by the unevenness in the sheet's metal coating surface. In general, the larger the plate volume penetrated by fields associated with the larger air gap, the greater the spatial expansion of the eddy currents in the plate. This means that the layer thickness is measured in a different area of the sheet depending on the air gap. Another aspect to consider is that the sheet metal sample holder sags because it is made of plastic, causing the sample to bend a little. This leads to a difference when compared with the analytical model, as there a flat sheet metal surface is assumed. This phenomenon has been simulated in a 2D FE simulation with a magnetically linear substrate and, therefore, constant permeability. This simulation was performed using FEMM and applying the same mesh rules as outlined in Section 3. In this simulation, however, the sheet metal shows a curvature that approximates the slight bending in the test bench. Applying the estimation approach to this simulation data, the layer thickness is then slightly overestimated, and the estimated layer thickness increases as the air gap increases. Thus, this theory can partially explain the tendency of the increasing coating thickness estimate with increasing air gap.

Another reason for the change in the estimated layer thickness with increasing air gap is the ferromagnetic substrate with a nonlinear B-H curve. This results in different magnetic

Table 3. Results of the coating thickness estimates and air gap estimates of the different sheet samples at the different air gaps considered

L/c	c_1 in µm	c_2 in µm	c_3 in µm
L = 3 mm	$\widehat{c}$ = 8.26 µm	$\widehat{c}$ = 11.68 µm	$\widehat{c}$ = 21.09 µm
	$\widehat{L}$ = 3.28 mm	$\widehat{L}$ = 2.99 mm	$\widehat{L}$ = 2.95 mm
L = 10 mm	$\widehat{c}$ = 9.16 µm	$\widehat{c}$ = 12.58 µm	$\widehat{c}$ = 21.73 µm
	$\widehat{L}$ = 10.68 mm	$\widehat{L}$ = 10.34 mm	$\widehat{L}$ = 10.12 mm
L = 20 mm	$\widehat{c}$ = 10.04 µm	$\widehat{c}$ = 14.05 µm	$\widehat{c}$ = 23.04 µm
	$\widehat{L}$ = 20.64 mm	$\widehat{L}$ = 20.20 mm	$\widehat{L}$ = 19.19 mm

Note: The values of the estimated coating thickness ĉ are given in micrometer and those of the estimated liftoff in millimeter
Source: Authors' own work

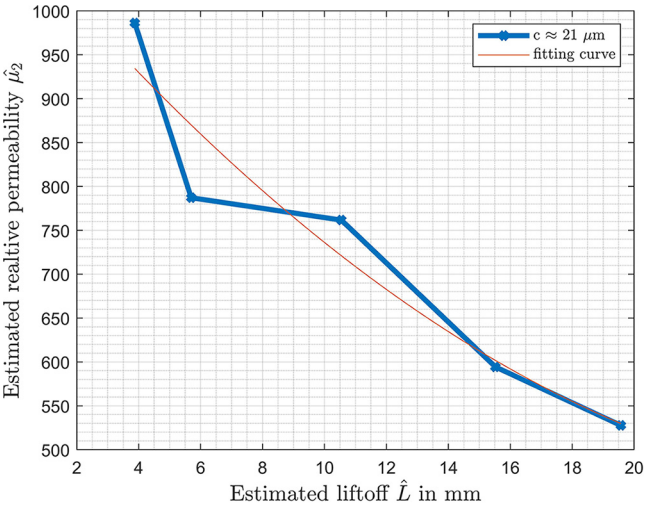

Source: Authors' own work

Figure 13. Results of the relative permeability estimation of a sheet metal sample with a coating thickness of $c \approx 21$ µm at different considered liftoffs

operating points for different air gaps, which influence the coating thickness estimation. This effect is also visible in the permeability estimate. It shows that the value of the estimated permeability $\widehat{\mu_2}$ decreases for increased air gap. This is due to the decreasing magnetic flux with increasing air gap and, thus, the shift of the magnetic operating point on the nonlinear material characteristics of the substrate. With a larger air gap, the magnetic field penetrating the material decreases, reducing the effective permeability. Estimating the effective permeability of a substrate with constant permeability from FE simulation data does not depend on whether the sheet is bent.

8. Conclusion

Using an eddy current sensor, this paper deals with the parameter determination of thin, electrically conductive and diamagnetic coatings on conductive and ferromagnetic steel substrates. The focus is on the determination of the coating thickness. In industrial processes, a relatively large air gap between the eddy current sensor and the object to be measured is often needed due to high process temperatures or air gap variations. Because a model-based estimation approach is used to determine the unknown sheet metal parameters, an analytical model known from the literature is verified by a 2D FE simulation for large air gaps. Generally, valid mesh rules for this type of eddy current problem are specified to obtain a relative error of less than 0.04% between the analytical model and the FE simulation, assuming sufficient radial sheet expansion, linear, isotropic and homogenous material. The required computing time stays under ten minutes per analyzed frequency. This also determines the minimum distance of the sensor system to the sheet's edge depending on the air gap to avoid an undesirable edge effect on the measuring voltage of the coil. Furthermore, a measurement setup is presented and applied, including the estimation of the unknown sheet metal material parameters and the liftoff. In contrast to many other studies, this approach does not use impedance analyzers for eddy

current testing. This allows selecting the excitation current and provides the opportunity to adjust the input power of the sensor system. Furthermore, this allows investigations regarding the influence of the magnetic nonlinearity of the substrate. Electrical steel sheets with silver ink coatings from 8 to 21 µm were studied in the test bench under consideration of air gaps between 3 and 20 mm. It is not possible to determine all parameters of the coated sheet independently of each other, based on simulation or measurement data. Therefore, it is assumed that the conductivities of the coating and the substrate are known in advance. The linear theory can be widely confirmed. However, the setting of different liftoffs and the associated different magnetic operating points lead to inaccuracies in the layer thickness estimation. With the presented setup, the coating thickness of the sheets studied can be determined to an accuracy of approximately ±2 µm for all air gaps under examination. This influence of the liftoff change on the layer thickness and permeability estimation is highlighted. The unwanted impact of nonlinear substrate material characteristics on parameter estimation is part of future research.

References

Cooley, J.W. and Tukey, J.W. (1965), "An algorithm for the machine calculation of complex Fourier series", *Mathematics of Computation*, Vol. 19 No. 90, pp. 297-301, doi: 10.1090/S0025-5718-1965-0178586-1.

DCP 520/84 HSR (2024), available at: www.servowatt.de/download/dcp_breitbandverstaerker.pdf

Dodd, D.L.S. (1969), *Some Eddy-Current Problems and Their Integral Solutions*, OAK RIDGE NATIONAL LABORATORY.

Koll, M., Wöckinger, D., Dobler, C., Goldbeck, G., Bramerdorfer, G., Schuster, S., Scheiblhofer, S., *et al*. (2024), "Investigations on eddy current sensors regarding inline-capability of zinc coating monitoring using a model-based estimator", *Journal of Magnetism and Magnetic Materials*, Vol. 592, p. 171754, doi: 10.1016/j.jmmm.2024.171754.

LOCTITE EDAG PF 410 E&C Datasheet (2024), available at: www.mouser.com/datasheet/2/773/LOCTITE_EDAG_PF_410_EC_en_US-2328171.pdf

Luquire, J.W., Deeds, W.E. and Dodd, C.V. (1970), "Alternating current distribution between planar conductors", *Journal of Applied Physics*, Vol. 41 No. 10, pp. 3983-3991, doi: 10.1063/1.1658399.

MathWorks, T.M. (2024), "MATLAB version: 9.6.0 (R20219a)", *The MathWorks Inc*, Natick, MA, United States.

Meeker, D. (2024), "FEMM manual".

Moriyasu, K., Kosaka, D., Kakishita, K., Hashimoto, M. and Koyama, F. (2018), "Measurement of plating thickness with high liftoff using eddy current testing", *Electromagnetic Non-Destructive Evaluation (XXI)*, IOS Press, pp. 263-268. doi: 10.3233/978-1-61499-836-5-263.

Moulder, J.C., Uzal, E. and Rose, J.H. (1992), "Thickness and conductivity of metallic layers from eddy current measurements", *Review of Scientific Instruments*, Vol. 63 No. 6, pp. 3455-3465, doi: 10.1063/1.1143749.

NI-USB–6356 (2024), available at: www.ni.com/docs/de-DE/bundle/pxie-usb-6356-specs/page/specs.html

Pauw, V.D. (1958), "A method of measuring the resistivity and Hall coefficient on lamellae of arbitrary shape", *Philips Tech. Rev*, Vol. 20, p. 220.

Ptchelintsev, A. and de Halleux, B. (1996), "Two-conductor line model: rapid inversion of eddy current data for foil thickness and conductivity determination", *Review of Scientific Instruments*, Vol. 67 No. 10, pp. 3688-3693, doi: 10.1063/1.1147136.

Ptchelintsev, A. and de Halleux, B. (1998), "Thickness and conductivity determination of thin nonmagnetic coatings on ferromagnetic conductive substrates using surface coils", *Review of Scientific Instruments*, Vol. 69 No. 3, pp. 1488-1494, doi: 10.1063/1.1148784.

Rayleigh, L. (1887), "XXV. Notes on electricity and magnetism.—III. On the behaviour of iron and steel under the operation of feeble magnetic forces", *The London, Edinburgh, and Dublin Philosophical Magazine and Journal of Science*, *Taylor and Francis*, Vol. 23 No. 142, pp. 225-245, doi: 10.1080/14786448708628000.

Sallen, R.P. and Key, E.L. (1955), "A practical method of designing RC active filters", *IRE Transactions on Circuit Theory, Presented at the IRE Transactions on Circuit Theory*, Vol. 2 No. 1, pp. 74-85, doi: 10.1109/TCT.1955.6500159.

Theodoulidis, T.P., Tsiboukis, T.D. and Kriezis, E.E. (1995), "Analytical solutions in eddy current testing of layered metals with continuous conductivity profiles", *IEEE Transactions on Magnetics*, Vol. 31 No. 3, pp. 2254-2260, doi: 10.1109/20.376236.

Uzal, E. and Rose, J.H. (1993), "The impedance of eddy current probes above layered metals whose conductivity and permeability vary continuously", *IEEE Transactions on Magnetics*, Vol. 29 No. 2, pp. 1869-1873, doi: 10.1109/20.250771.

Author affiliations

Martin Koll, Daniel Wöckinger, Christoph Dobler, Gereon Goldbeck and Gerd Bramerdorfer, Institute of Electric Drives and Power Electronics, Johannes Kepler University Linz, Linz, Austria, and

Stefan Schuster, Stefan Scheiblhofer, Norbert Gstöttenbauer and Johann Reisinger, voestalpine Stahl GmbH, Linz, Austria

Corresponding author
Martin Koll can be contacted at: martin.koll@jku.at